X-Ray, Proton, and Electron Radiation Effects on Type I Fiber Bragg Gratings

Thomas Blanchet, Adriana Morana, Timothé Allanche, Camille Sabatier, Imène Reghioua, Emmanuel Marin, Aziz Boukenter, Youcef Ouerdane, Philippe Paillet, Marc Gaillardin, et al.

X-ray, Proton and Electron Radiation Effects on Type I Fiber Bragg Gratings

Thomas Blanchet, *Student Member, IEEE,* Adriana Morana *Member, IEEE,* Timothé Allanche, *Student Member, IEEE,* Camille Sabatier, *Student Member, IEEE,* Imène Reghioua, *Student Member, IEEE,*, Emmanuel Marin, Aziz Boukenter, Youcef Ouerdane, Philippe Paillet, *Fellow IEEE,* Marc Gaillardin, *Member, IEEE,* Olivier Duhamel, Claude Marcandella, M. Trinczek, Gilles Assaillit, G. Auriel, D. Aubert, Guillaume Laffont, and Sylvain Girard, *Senior Member, IEEE*

Abstract— Fiber Bragg Gratings (FBGs) are one of the most used optical fiber sensors and they have recently drawn the attention of several research groups for their potential applications in harsh radiation environments. Up to now, their performances have been mainly evaluated under ionizing radiations, such as X- or γ-rays. We compare here the effects of different irradiation types, including X-rays, protons and electrons, on type I FBGs written by UV laser exposure in Ge, P/Ce and B/Ge doped single-mode optical fibers. Different irradiation conditions were used according to the sources. 6 MeV electron irradiations were performed at a dose-rate of 120 Gy(SiO_2)/s up to an accumulated dose of 500 kGy; whereas for the 63 MeV protons the estimated equivalent dose-rate was of 0.75 Gy(SiO_2)/s up to a total dose of 7 kGy. In order to compare their effects with those induced by X-rays, two irradiations with 45 keV photons were performed with different dose-rates (0.75 and 60 Gy/s (SiO_2)) up to a total dose of 10 kGy and 500 kGy, respectively. We demonstrated that X-rays and protons induce comparable effects at doses of about 10 kGy, whereas the behavior under electron beam appears to be strongly dependent on the fiber composition. For example, the grating in the B/Ge co-doped fiber is the most sensitive to electrons and the most resistant to X-rays; whereas the FBG inscribed in the H_2-loaded P/Ce co-doped fiber has exactly the opposite behavior.

***Index Terms*— X-rays, protons, electrons, Fiber Bragg Grating, Optical fiber sensors, Optical Fibers**

Manuscript received September 30th, 2017. Manuscript received for revision December 19th 2017. Final acceptance March 28th 2018

T. Blanchet, A. Morana, T. Allanche, E. Marin, A. Boukenter, Y. Ouerdane and S. Girard are with Univ-Lyon, Laboratoire Hubert Curien, CNRS UMR 5516, 42000 Saint-Etienne, France, phone : (+33)469 663 269; email: thomas.blanchet@univ-st-etienne.fr

T. Blanchet and G. Laffont are with the French Alternative Energies and Atomic Energy Commission , LIST, LCAE, 91191 Gif-sur-Yvette, France

P. Paillet, M. Gaillardin, O. Duhamel, C. Marcandella are with the French Alternative Energies and Atomic Commission, CEA, DAM, DIF, 91297 Arpajon, France

M. Trinczek is with TRIUMF Laboratory, 4004 Westbrook Mall, Vancouver, Canada.

G. Assaillit, G. Auriel and D. Aubert are with the French Alternative Energies and Atomic Commission (CEA), CEA DAM Gramat, France

I. Introduction

OVER the last decades, the performances of Optical Fiber-based Sensors (OFSs) in radiation environments have been investigated by numerous research groups, because of all the advantages the OFSs offer for such environments as their small size, light weight, their multiplexing capability and their electromagnetic immunity. Among the different classes of OFSs, the Fiber Bragg Grating (FBG) technology is the most studied one and is regularly used for structural health monitoring in civil, military and oil and gas applications [1],[2].

A FBG consists of a periodic modulation along a few mm fiber length of the refractive index of its core. The fabricated grating induces a reflection of particular wavelengths. This reflection is centered around the Bragg wavelength (λ_B). The FBG acts as a filter, which is a pass-band in reflection and a band-stop in transmission. The Bragg wavelength λ_B is defined as:

$$\lambda_B = 2\, n_{eff}\, \Lambda \qquad (1)$$

with n_{eff} the effective refractive index and Λ the grating period. When temperature and/or strain are applied to a FBG, λ_B shifts and this wavelength difference can be used to monitor the external parameter variations. The Bragg wavelength depends linearly on the temperature between 20°C and 100°C, indeed:

$$\lambda_B(T) = \lambda_B(T_0) + \alpha\,(T - T_0) \qquad (2)$$

where T_0 is a reference temperature and α is the FBG temperature sensitivity coefficient, whose value is about 10 pm/°C for silica based fibers and depends on their composition, opto-geometry, FBG laser inscription conditions and pre- or post-treatments of the fiber or the grating [3].

Under radiation, three main macroscopic phenomena can be observed in silica based fibers [4]. The first one is the well-known Radiation Induced Attenuation (RIA), which is due to absorption bands related to radiation induced defects through ionization or knock-on processes. The second effect is the Radiation Induced Emission (RIE) from pre-existing and/or radiation-induced defect centers excited by radiation or through Cerenkov effect, if the incident particle energy is sufficient. The

last mechanism is the Radiation Induced Compaction (RIC) that corresponds to a change in the silica density [4], [5], [6]. Both RIA and RIC cause refractive index variations, through the Kramers-Kronig relation and Lorentz-Lorenz equation, respectively. Consequently, the FBG sensing performances are influenced by radiation [1]. Indeed, radiation can change the effective refractive index (Δn_{eff}), the amplitude of the refractive index modulation (Δn^{mod}) and the grating period ($\Delta\Lambda$), causing a reduction of the maximum peak reflectivity, which implies a signal-to-noise ratio reduction as well as a radiation-induced Bragg wavelength shift (RI-BWS, $\Delta\lambda_B$), as [1]:

$$\frac{\Delta\lambda_B}{\lambda_B} = \frac{\Delta n_{eff}}{n_{eff}} + \frac{\Delta\Lambda}{\Lambda} \qquad (3)$$

This RI-BWS causes a direct error on the temperature and/or strain measurements and should be minimized as much as possible. For example, a refractive index change of 10^{-4} can shift the Bragg Wavelength by about 100 pm, which corresponds to an error close to 10°C on the temperature [1].
It has been demonstrated that the fiber composition [7], the grating inscription techniques [8] and the post-inscription temperature annealing [9] can modify FBG response under ionizing radiation. For example, Henschel *et al.* have shown that the FBG radiation hardness is not directly related to the fiber used for the inscription i.e. a radiation hardened fiber will not lead automatically to a FBG radiation hardened against RI-BWS [7].

When dealing with space applications, also the presence of particles, as electrons and protons, has to be taken into account [10], [11]. Consequently it is very pertinent to characterize their effects on FBG response and to compare them with the degradation induced by other radiation types, since until today almost no study on the effects of such kinds of irradiations is present in the literature. Curras *et al.* [12] investigated the effects induced by a proton beam on recoated FBGs and they stated that acrylate coating gives rise to a more radiation resistant grating to proton irradiation; whereas the ormocer coated FBGs appear as the most sensitive. Same conclusions were obtained by Gusarov *et al.* [13] for the gamma-ray induced effects on recoated gratings. The coating influence is not here reported for our FBGs as for some of the targeted applications, the FBGs are not recoated before their integration in more complex sensor architectures. For the other applications, it appears as mandatory to perform a complete study of the impact of the various coatings from acrylate to polyimide ones.

In this paper, we study the effects of electron and proton irradiations on uncoated FBGs and we compare them with the effects induced by X-rays. All the investigated FBGs are Type I [14], written with a continuous wave (CW) UV laser at 244 nm in single-mode optical fibers characterized by different core dopants that render them photosensitive: Germanium, Bore/Germanium and Phosphorus/Cerium.

II. Experimental Procedure

Several Type I FBGs were written at the Laboratory Hubert Curien (LabHC, Saint Etienne, France) in the four selected acrylate coated fibers. Their main characteristics are reported in Table I. In order to enhance the fiber photosensitivity, before the inscription a pre-H_2-loading was performed at 150 bars and Room Temperature (RT) for a week on all the fibers except the B/Ge. This treatment allows to increase the photosensitivity of the fiber by saturating the core with hydrogen.

FBGs of 5 mm length were inscribed at RT using the Lloyd mirror technique by continuous wave (CW) double-frequency Argon laser (MotoFred from Coherent), operating at 244 nm with an optical power of 120 mW. Before inscription, the fiber coating was mechanically stripped in the zone of the FBG inscription and never restored. The initial reflectivity of all the gratings was about 90% (-10 dB of amplitude in transmission). After the inscription, the gratings were subjected to an 8 hour lasting thermal treatment at 120°C, to ensure the outgassing of the residual hydrogen and to stabilize the FBGs at temperatures below 120°C.

TABLE I
LIST OF TESTED FIBERS

Fiber	Composition		H_2	FBGs	
	Core	Cladding		λ_B (nm)	FWHM (nm)
Ge (High Content)	Ge >15 wt%	Pure silica	yes	1550	1.0
Ge (Low Content)	Ge ~5wt%	Pure silica	yes	1550	0.5
B/Ge	Ge ~10 wt% B ~20wt% P~8 wt%	Pure silica	no	1549	0.04
P/Ce	Ce (below EDX detection limit).	Pure silica	yes	1548	0.6

The bare FBGs were fixed stress-free on aluminum plates, thanks to grooves engraved on them and aluminum bridles, except for the electron irradiations where the FBGs were vertically hung inside the electron beam, in order to avoid the effects induced by electrons on the aluminum plate.

The FBG reflection spectra were monitored in parallel with two acquisition systems, depending on the irradiation test (see Fig. 1):

- a Fabry-Perot cavity (National Instrument PMA 1115) with a resolution of 4 pm with a maximum optical power of 0.25 mW between 1510 and 1590 nm for the X-ray irradiation;
- a tunable laser source (Tunics Plus, NetTest) with a maximal optical power of 10 mW in a range of 1500 nm and 1630 nm, an optical tester with a 1 pm wavelength resolution (Optics Yenista CT400), a coupler and four circulators, for the proton and electron irradiations.

The stabilities of the acquisition systems were tested before the radiation tests. No input power instability, nor wavelength shift were observed for several days. For the Tunics/CT 400 devices, no time drift can appear since the direct output of the tunable laser is scanned at the same time than the four channels. The two measurement systems have a good repeatability when we irradiated FBGs under X-rays (less than 5%).

At least two thermocouples were used to monitor the

temperature, in order to isolate the RI-BWS from the contribution induced by temperature variations. The Bragg position was determined as the average of the wavelength values at half maximum.

The proton irradiation was performed at the Proton Irradiation Facility (PIF) of TRIUMF Laboratory (Vancouver, Canada). The proton energy was 63 MeV and the flux was about 8×10^5 p/(cm^2·s), which corresponds to an equivalent dose-rate of about 0.75 Gy(SiO_2)/s. The irradiation lasted three or four hours, to reach an accumulated equivalent dose higher than 7 kGy(SiO_2). The temperature was stable at around 26°C during the runs with fluctuations lower than 0.2°C resulting in BWS smaller than 2 pm comparable to our experimental uncertainties.

The electron irradiation was performed at the Oriatron facility of CEA in Gramat (France). The facility delivers 6 MeV electrons [15] accelerating linearly the electrons by using a Radio Frequency Electromagnetic Wave in a specific cavity. It can operate in various configurations: a single pulse or in burst mode or in quasi-continuous mode at a frequency of 250 Hz. The duration of each pulse is 4.5 µs and the dose rate is 14 kGy/min at a distance of 1 m. At this distance, the beam diameter is equal to 11.5 cm with a divergence of 17°. During the experiments we used the quasi-continuous mode.

The dose rate for this experiment was of about 120 Gy(SiO_2)/s, which corresponds to a distance of 1.9 m between the irradiation source and the gratings, allowing to reach an accumulated dose of 500 kGy(SiO_2). The temperature recorded by the thermocouples increases from RT up to about 35°C during irradiation, but because of the electrons, an error of 1°C is associated to the thermocouple temperature values, which corresponds to an error of 10 pm on the FBG response; this is due to the high flux of electrons during irradiation, which interferes with the temperature measurement by adding some capacity charge.

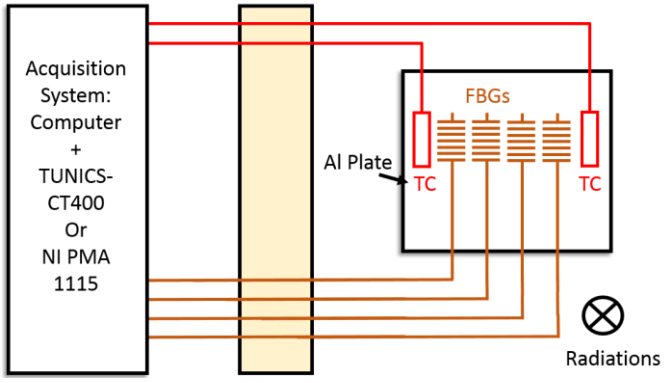

Fig. 1. Experimental setup used to characterize the FBG response at the different facilities. FBGs are fixed stress-free on an Aluminium plate with two reference thermocouples (TC) – except for the electron radiation where the FBG were vertically exposed. Radiation beam is perpendicular to the FBGs, which are interrogated either by a NI PMA 1115 for the X- irradiations or by a YENISTA CT400 with a Tunable Laser TUNICS Plus for the proton and electron irradiations.

X-ray irradiation were performed at the Laboratoire Hubert Curien with the MOPERIX machine, whose X-ray mean energy is around 45 keV. In order to compare the effects induced by X-rays and those by protons or electrons, the dose rate was fixed at 0.75 Gy(SiO_2)/s and 60 Gy/s and the total ionizing dose (TID) was 10 kGy(SiO_2) and 500 kGy, respectively. The temperature variations were less than 2°C and 5°C for the first and second dose-rate, respectively.

In the following sections, the BWS induced by temperature variations were subtracted from the recorded shift, in order to highlight only the RI-BWS. The temperature induced BWS was calculated by using the temperature coefficient measured before irradiation, not affected by X-rays and slightly affected by electrons (α variation within 7%).

III. Results

The results will be discussed with regards to the fiber composition in the next sections. All the measurements have been made in-situ meaning during the irradiation runs.

A. FBGs behavior under radiation

Under irradiation, two main effects can be observed. The first one is a reduction of the peak amplitude and the second one is a shift of the Bragg wavelength as clearly highlighted in Fig 2.

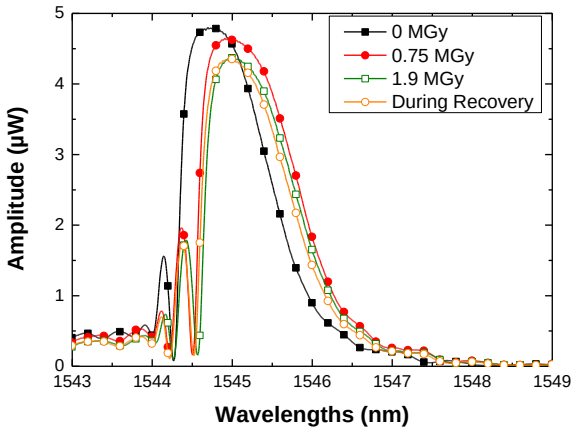

Fig. 2. Reflection spectra of a grating inscribed in the Ge low content fiber, before and after irradiation (dose-rate being 80 Gy/s) at 0.75 MGy and 1.9 MGy

Figure 2 shows the changes induced by X-rays on the reflection spectrum of a FBG inscribed on Ge low content fiber. The Bragg wavelength shift here is due to radiation at different dose levels (0.75 and 1.9 MGy) and to temperature variation (less than 10°C). The amplitude variation is due to radiations. Two effects are responsible of a decrease of at least 9% the maximum peak amplitude: the RIA and an effective refractive index change. With the irradiation the effective refractive index can decrease and leads to a decrease of the FBG peak amplitude. The RIA of the Ge low content fiber is of about a few hundredths of dB/km in this spectral domain and can contribute to the FBG erasing [16].

TABLE II
THERMAL SENSITIVITY COEFFICIENTS BEFORE AND AFTER IRRADIATION

Fibers	Before	After irradiation					
		Protons		Electrons		X-rays	
	α (pm/°C)	*α (pm/°C)*	δ (%)	*α (pm/°C)*	δ (%)	*α (pm/°C)*	δ (%)
Ge (low content)	10.2	10.2	0			10.2	0
Ge (High Content)	10.3					10.2	1
B/Ge	8.8			8.7	1	8.9	1
P/Ce	10.2			9.5	7	10.9	7

B. Comparison of the thermal sensitivity coefficient before and after the irradiations.

During all the electron and X-ray irradiations, the gratings were corrected in temperature in order to only obtain the radiation effects. Before and after irradiation, the thermal sensitivity coefficients were calculated with (1) by placing the gratings inside an oven up to 80°C and by recording their spectra and monitoring the temperature with two thermocouples.

Table II reports the thermal coefficients calculated before and after irradiation. We do not have the results for all the gratings, for example, no data is available for the gratings inscribed in the Ge-doped fibers under electron irradiations, since these gratings did not survive after the experiments. For the proton irradiation, the BWS was not corrected in temperature since the temperature variations were below 2°C which represents an error of 2 pm on the results. However, the accumulated dose was low (>10 kGy), and as expected, no change in the thermal coefficient was observed for the grating inscribed in the Ge low content.

For the X-ray or electron irradiations, a variation of less than 1% is observed for the Ge-doped or B/Ge co-doped fibers.

Instead, for the FBGs written in the P/Ce co-doped fibers, a variations of almost 7% is observed, with X-ray or electron irradiations. However, such variation does not change the conclusions on the following paragraphs.

For all the following results, all the BWSs were corrected with the thermal sensitivity coefficient value calculated before the irradiations. On the following graphs, the Y-axis "temperature error" was calculated with a mean thermal coefficient of 10 pm/°C.

The next figures report only the RI-BWSs.

C. FBGs written on Ge-doped fibers

Fig. 3 compares the RI-BWS induced by protons with those induced by X-rays on FBGs inscribed in two H_2-loaded Ge-doped fibers differing by their Ge content (5 wt% and more than 15 wt%). For both irradiations, the equivalent dose-rate was about 0.75 Gy/s and the TID exceeded 7 kGy.

First, we note that, as for X- or γ-irradiations [1], during the proton irradiation the Bragg wavelength shifts towards the larger values. Nevertheless, the BWS induced by X-rays is larger than that induced by protons by a factor of about 1.5. Such a result was unexpected, considering that protons can generate defects also through knock-on processes and not only through ionization, as X-rays.

However, it is known that the RI-BWS increases by increasing the dose-rate. Indeed, by comparing the proton induced BWS with those recorded for X-ray irradiation performed at dose-rates below 0.75 Gy/s, we observed a good agreement between the proton and X-ray results. The observed difference corresponds to an error on the dose-rate estimation of about 15%, which is completely reasonable by taking into account the errors made on the estimation of the dose-rate for both X-ray and proton irradiation and by knowing that the proton beam flux is not stable for experiments lasting as much as four hours. Finally, concerning the dependence of RI-BWS to the Ge concentration, the higher the Ge concentration, the larger seems the RI-BWS [17], [18].

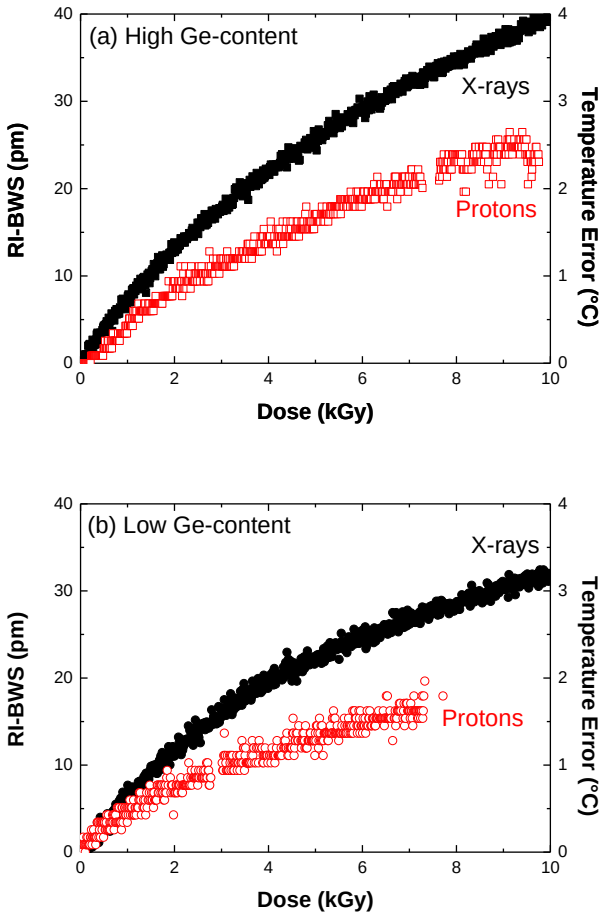

Fig. 3. RI-BWS of FBGs inscribed in two types of H_2-loaded Ge-doped fibers differing by their Ge concentration of (a) high and (b) low content, under X-rays (full black squares) and proton irradiations (empty red circles) at 0.75 Gy/s, up to a total dose of ~10 kGy. On the right vertical axis are reported the equivalent radiation-induced errors on the temperature measurements.

Fig. 4 compares the effects of electrons (120 Gy/s) and X-rays (60 Gy/s). As mentioned above, the shift induced by X-rays at 120 Gy/s dose-rate should be larger than that induced at 60 Gy/s. However, as highlighted in [18], the value of the RI-BWS saturation shows itself a saturation behavior with the dose-rate: this is reached for dose-rates as high as 50 Gy/s. Consequently, no effect induced by the dose-rate is expected between the results recorded during X-rays or electron irradiations.

Under X-rays, the Bragg wavelength of both FBGs increases with the dose without saturating at 500 kGy. Moreover, the dependence of the RI-BWS on the Ge concentration is preserved also for these high dose-rate X-ray irradiation.

During the electron irradiation, the RI-BWS shows a saturation behavior at about 170 pm for both gratings, independently on their Ge concentrations.

By comparing the results for the X-ray and electron irradiations, no effect is observed for the FBG on the low-Ge doped fiber (Fig. 4 (b)), whereas for the FBG written in the highly Ge-doped fiber, X-rays induce a larger shift than electrons at the same dose: the recorded BWS at 500 kGy is 230 pm for the X-rays and only 160 pm for the electrons.

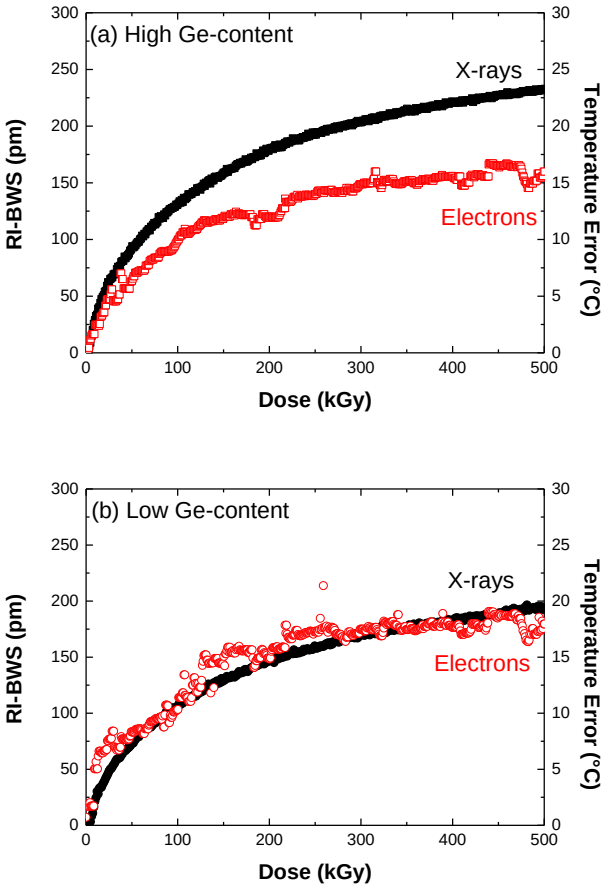

Fig. 4. RI-BWS of FBGs inscribed in two types of H_2-loaded Ge-doped fibers differing by their Ge concentration of (a) high and (b) low content, under X-rays (full black squares) and electron irradiations (empty red circles) at 60 and 120 Gy/s dose-rate, respectively, up to a total dose of 500 kGy. On the right vertical axis are reported the equivalent radiation-induced errors on the temperature measurements.

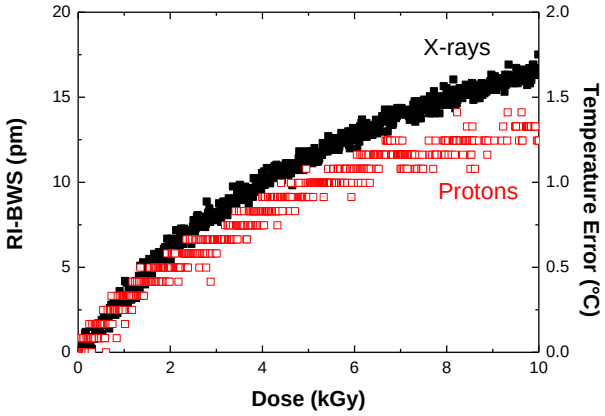

Fig. 5. RI-BWS of FBG written in a B/Ge co-doped fiber, under X-rays (full black squares) and proton irradiations (empty red circles) at 0.75 Gy/s dose-rate, up to a total dose of almost 10 kGy. On the right vertical axis are reported the equivalent radiation-induced errors on the temperature measurements.

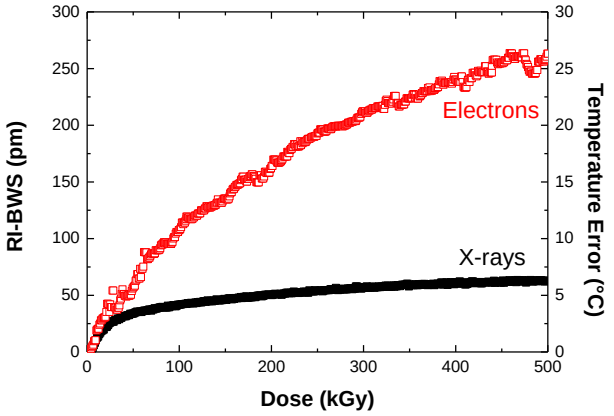

Fig. 6. RI-BWS of a FBG written in a B/Ge co-doped fiber, under X-rays (full black squares) and electron irradiations (empty red circles) at 60 and 120 Gy/s dose-rate, respectively, up to a total dose of 500 kGy. On the right vertical axis are reported the equivalent radiation-induced errors on the temperature measurements.

D. FBGs written on B/Ge co-doped fibers

Fig. 5 compares the effects of protons and X-rays on the response of the FBG written in the B/Ge co-doped fiber and leads to the same conclusion stated for the gratings in the Ge-doped fibers. A similar behavior is induced by X-rays and protons; the observed difference remains within our experimental uncertainties regarding the dose-rate estimation and measurements.

Fig. 6 compares the effects of electrons and X-rays for the FBG inscribed in the B/Ge fiber. Contrary to the results obtained for the FBGs in the H_2-loaded Ge-doped fibers, electrons induce a larger shift than X-rays, even at low doses. Indeed, at 50 kGy the recorded shift is 30 pm under X-rays compared to more than 50 pm for electrons. This difference increases as the dose increases and at 500 kGy accumulated dose the shift reaches 60 pm and 260 pm for X-ray and electron irradiation, respectively. This behavior could be associated to the Boron presence (20 wt%), since this fiber has a Ge concentration of 10 wt%, which is between the concentration of

Ge in the fiber low content (5 wt%) and high content (15 wt%). In the last two fibers, a saturation effect is observed at 170 pm under electron exposure.

Therefore, the grating written in a highly photosensitive B/Ge co-doped fiber is more sensitive to electrons than to X-rays, regardless of the accumulated dose up to 500 kGy. But, this FBG has the same behavior under protons and X-rays up to a TID of 10 kGy, taking into account the measurement accuracy.

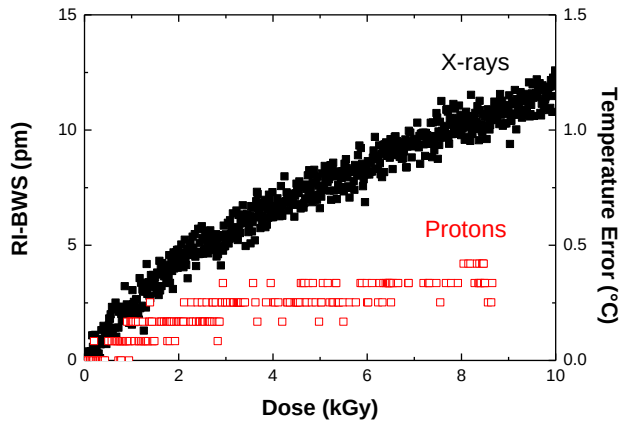

Fig. 7. RI-BWS of FBG written in a H_2-loaded P/Ce co-doped fiber, under X-rays (full black squares) and proton irradiations (empty red circles) at 0.75 Gy/s dose-rate, up to a total dose of almost 10 kGy. On the right vertical axis are reported the equivalent radiation-induced errors on the temperature measurements.

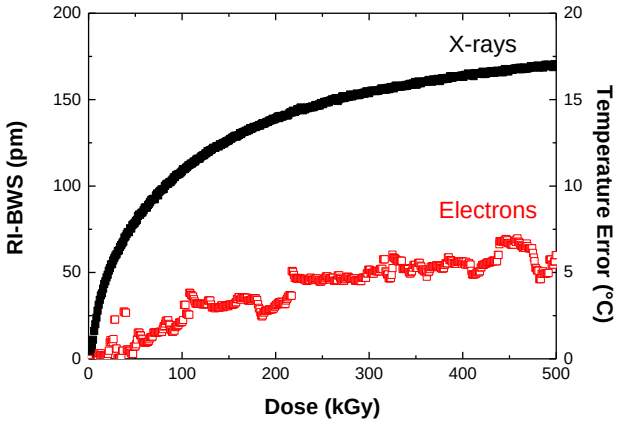

Fig. 8. RI-BWS of a FBG written in a H_2-loaded P/Ce co-doped fiber, under X-rays (full black squares) and electron irradiations (empty red circles) at 60 and 120 Gy/s dose-rate, respectively, up to a total dose of 500 kGy. On the right vertical axis are reported the equivalent radiation-induced errors on the temperature measurements.

E. FBGs written on P/Ce co-doped fibers

Fig. 7 highlights the effects of X-rays and protons on the response of the FBG written in the P/Ce co-doped fiber. Contrary to the other FBGs, the Bragg wavelength of this grating does not shift significantly as a function of proton irradiation; indeed during the entire test the RI-BWS is less than 4 pm, which corresponds to an error on the temperature measurement lower than 0.5°C. A larger shift is, instead, highlighted during the X-ray irradiation and a clear dependence on the accumulated dose can be observed. Moreover, the RI-BWS is lower for this grating than for the others.

Finally, Fig. 8 gives the results of the X-ray and electron irradiation of a grating inscribed a P/Ce fiber. In comparison to the grating in the B/Ge co-doped fiber, a larger shift is recorded under X-rays than under electrons. Indeed, at 500 kGy TID the RI-BWS is 170 pm for X-rays and only about 50 pm for the electrons. Even at low doses, the two gratings show a completely different behavior.

IV. Discussion

The here reported results clearly show different FBG responses under different types of radiations and for different fiber compositions. Tables III and IV show the RI-BWS values recorded at the maximum accumulated doses, that is 10 kGy and 500 kGy for the proton and electron irradiations, spectively, and their comparison with the equivalent X-ray test results.

First, no big difference can be observed on the effects of protons and X-rays on all the FBGs, within a reasonable error, even if the protons are more energetic (63 MeV) compared to X-rays (45 keV) and they can cause knock-on processes and compaction in the fibers, whereas X-rays generate defects only through ionization.

Table III
Comparison of RI-BWS at TID of about 7 kGy, under X-ray and Proton Irradiation

Fiber composition	X-ray induced BWS at 7 kGy (pm)	Proton induced BWS at 7 kGy (pm)
Ge (High Content)	30 ± 2	22 ± 2
Ge (Low Content)	27 ± 2	17 ± 2
B/Ge	14 ± 2	13 ± 2
P/Ce	7 ± 2	4 ± 1

Moreover, the FBG written in the P/Ce co-doped fiber does not seem to be affected by the protons up to 10 kGy. Under electron irradiation, each grating shows a different behavior.

Table IV
Comparison of RI-BWS at TID of about 500 kGy, under X-ray and Electron Irradiation

Fiber composition	X-ray induced BWS at 500 kGy (pm)	Electron induced BWS at 500 kGy (pm)
Ge (High Content)	230 ± 2	170 ± 10
Ge (Low Content)	190 ± 2	170 ± 10
B/Ge	60 ± 2	260 ± 10
P/Ce	170 ± 2	55 ± 10

Among all the studied gratings, the one written inside the B/Ge co-doped fiber is the most sensitive to the electron beam and the least sensitive to the X-rays, at high dose-rate. This behavior can be associated to the boron presence.

The FBG in the H_2-loaded P/Ce co-doped fiber is the most resistant to both electrons and protons, but not to X-rays.

Finally, concerning the gratings in the H_2-loaded Ge-doped fibers, the RI-BWS increases with the Ge concentration under X-rays, whereas it is not dependent on this during the electron irradiations. Moreover, for the fiber with low Ge content, no significant difference is observed between X-ray and electron irradiation.

V. Conclusion

In this paper, we compared the effects induced on type I UV-FBGs by three different kinds of radiation: X-rays, protons and electrons.

Up to the accumulated dose of 10 kGy, X-rays and protons induce comparable BWSs of the gratings in the Ge-doped or B/Ge co-doped fibers. The FBG in the P/Ce fiber is resistant to the proton irradiation.

Regarding electron irradiation, different responses are obtained for the different gratings. For example, the FBG written inside the B/Ge co-doped fiber is the most sensitive to the electron beam and the most resistant to X-rays; whereas the grating in the H_2-loaded P/Ce co-doped fiber has exactly the opposite behavior. The effects induced by electrons and X-rays, instead, are comparable for the gratings inside H_2-loaded Ge-doped fibers.

To conclude, both the fiber composition and the nature of radiation strongly influence the FBG response. It appears then as mandatory to perform the radiation qualification tests on the FBGs using the nature of particles expected in the environment of interest. Further studies will be performed to understand the mechanisms explaining the observed difference in the radiation response of some of the tested FBGs.

In order to better understand the influence of the irradiation nature and the relative contributions of ionizing and displacement damages on the FBG RI-BWS, a more systematic study will have to be performed in the future with electrons, protons and also neutrons, varying also the energy of these particles whenever possible.

References

[1] A. Gusarov and S. K. Hoeffgen, "Radiation Effects on Fiber Gratings," *IEEE Trans. Nucl. Sci.*, vol. 60, no. 3, pp. 2037–2053, Jun. 2013.

[2] P. Ferdinand, S. Magne, and G. Laffont, "Optical Fiber Sensors to improve the safety of Nuclear Power Plants," in 4th Asia Pacific Optical Sensors Conference, Wuhan, China, 2013, doi: 10.1117/12.2033922

[3] J. Canning, "Fibre gratings and devices for sensors and lasers," *Laser Photonics Rev.*, vol. 2, no. 4, pp. 275–289, Aug. 2008.

[4] S. Girard *et al.*, "Radiation Effects on Silica-Based Optical Fibers: Recent Advances and Future Challenges," *IEEE Trans. Nucl. Sci.*, vol. 60, no. 3, pp. 2015–2036, Jun. 2013.

[5] W. Primak, "Fast-neutron-induced changes in quartz and vitreous silica," *Phys. Rev.*, vol. 110, no. 6, pp. 1240–1254, 1958.

[6] L. Remy, G. Cheymol, A. Gusarov, A. Morana, E. Marin, and S. Girard, "Compaction in Optical Fibres and Fibre Bragg Gratings Under Nuclear Reactor High Neutron and Gamma Fluence," *IEEE Trans. Nucl. Sci.*, vol. 63, no. 4, pp. 2317–2322, Aug. 2016.

[7] H. Henschel, S. K. Hoeffgen, K. Krebber, J. Kuhnhenn, and U. Weinand, "Influence of Fiber Composition and Grating Fabrication on the Radiation Sensitivity of Fiber Bragg Gratings," *IEEE Trans. Nucl. Sci.*, vol. 55, no. 4, pp. 2235–2242, Aug. 2008.

[8] A. Morana *et al.*, "Influence of photo-inscription conditions on the radiation-response of fiber Bragg gratings," *Opt. Express*, vol. 23, no. 7, pp. 8659–8669, Apr. 2015.

[9] A. Morana *et al.*, "Radiation tolerant fiber Bragg gratings for high temperature monitoring at MGy dose levels," *Opt. Lett.*, vol. 39, no. 18, pp. 5313–5316, Sep. 2014.

[10] "Survivable Systems for Extreme Environments | Science and Technology." [Online]. Available: https://scienceandtechnology.jpl.nasa.gov/research/research-topics-list/spacecraft-technologies/survivable-systems-extreme-environments. [Accessed: 18-Apr-2017].

[11] J. D. Cressler and H. A. Mantooth, *Extreme environment electronics*. CRC Press, 2012.

[12] E. Curras *et al.*, "Influence of the Fiber Coating Type on the Strain Response of Proton-Irradiated Fiber Bragg Gratings," *IEEE Trans. Nucl. Sci.*, vol. 59, no. 4, pp. 937–942, Aug. 2012.

[13] A. Gusarov, C. Chojetzki, I. Mckenzie, H. Thienpont, and F. Berghmans, "Effect of the Fiber Coating on the Radiation Sensitivity of Type I FBGs," *IEEE Photonics Technol. Lett.*, vol. 20, no. 21, pp. 1802–1804, Nov. 2008.

[14] G. Meltz, W. Morey, and W. H. Glenn, "Formation of Bragg gratings in optical fibers by a transverse holographic method," *Opt. Lett.*, vol. 14, no. 15, pp. 823–825, 1989.

[15] D. Aubert et al., "A 6 MeV electron Linac facility for mutlipurpose radiation testing," 2016 RADECS Proceedings, doi: 10.1109/RADECS.2016.8093158

[16] S. Rizzolo *et al.*, "Radiation effects on optical frequency domain reflectometry fiber-based sensor," *Opt. Lett.*, vol. 40, no. 20, pp. 4571–4574, Oct. 2015.

[17] S. Lin, N. Song, J. Jin, X. Wang, and G. Yang, "Effect of Grating Fabrication on Radiation Sensitivity of Fiber Bragg Gratings in Gamma Radiation Field," *IEEE Trans. Nucl. Sci.*, vol. 58, no. 4, pp. 2111–2117, Aug. 2011.

[18] A. Morana *et al.*, "Dose Rate Effect Comparison on the Radiation Response of Type I Fiber Bragg Gratings Written With UV cw Laser," *IEEE Trans. Nucl. Sci.*, vol. 63, no. 4, pp. 2046–2050, May 2016.